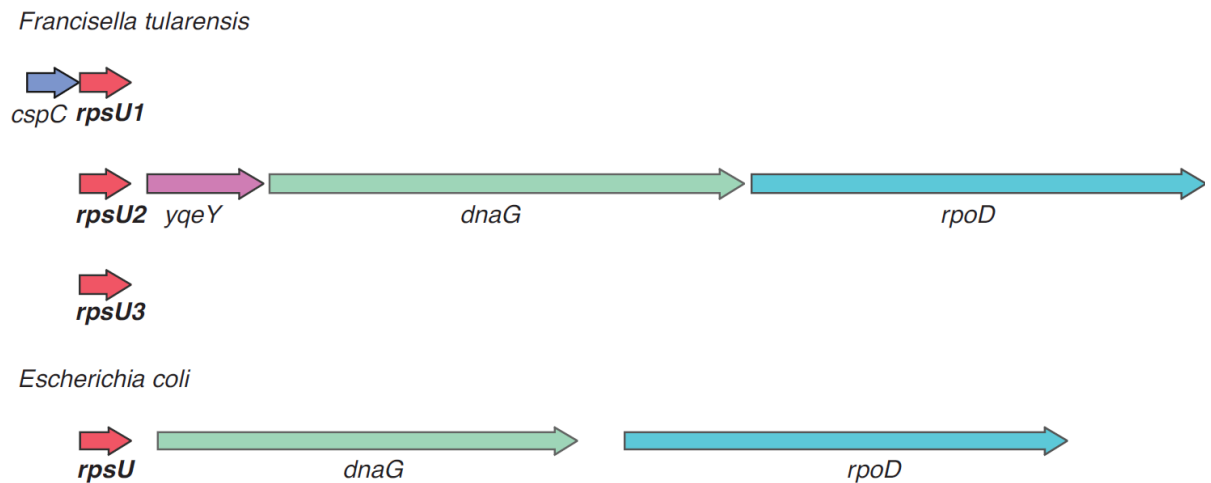


## SUPPLEMENTAL FIGURES



**Figure S1. *F. tularensis* encodes three *rpsU* genes.** *F. tularensis* *rpsU2*, which encodes bS21-2, is syntenic with the only *rpsU* in *E. coli*, which is located in the macromolecular synthesis operon (1). This operon in *E. coli* includes *rpsU* (encoding bS21), *dnaG* (encoding DNA primase), and *rpoD* (encoding RNA polymerase  $\sigma^{70}$ ). In *F. tularensis*, this operon also includes *yqeY*, the product of which may be involved in tRNA aminoacylation. *rpsU1*, encoding bS21-1, is located immediately downstream of *cspC* (encoding cold-shock protein CspC), while *rpsU3*, encoding bS21-3, is not apparently in an operon with other genes. Genomic locations of *rpsU* genes were determined using RefSeq NC\_007880 for *F. tularensis* and NC\_000913 for *E. coli*.

	<i>F. tularensis</i> subsp <i>holarctica</i> LVS bS21-1	<i>F. tularensis</i> subsp <i>holarctica</i> LVS bS21-3	<i>F. tularensis</i> subsp <i>holarctica</i> LVS bS21-2	<i>E. coli</i> bS21
<i>F. tularensis</i> subsp <i>holarctica</i> LVS bS21-1	100.0	72.3	54.0	50.8
<i>F. tularensis</i> subsp <i>holarctica</i> LVS bS21-3		100.0	47.6	48.5
<i>F. tularensis</i> subsp <i>holarctica</i> LVS bS21-2			100.0	60.0
<i>E. coli</i> bS21				100.0

**Figure S2. The three bS21 homologs in *F. tularensis* are distinct.** Percent identities of amino acid sequences for *F. tularensis* LVS bS21-1, bS21-2, bS21-3 and *E. coli* bS21 were calculated using the multiple sequence alignment tool ClustalOmega (2). The bS21 homologs in *F. tularensis* are similar to each other, particularly bS21-1 and bS21-3 which are 72% identical at the amino acid level. bS21-2, encoded by the *rpsU* homolog gene syntenic to the single *E. coli rpsU* gene, is also the most similar to *E. coli* bS21, with 60% amino acid identity.

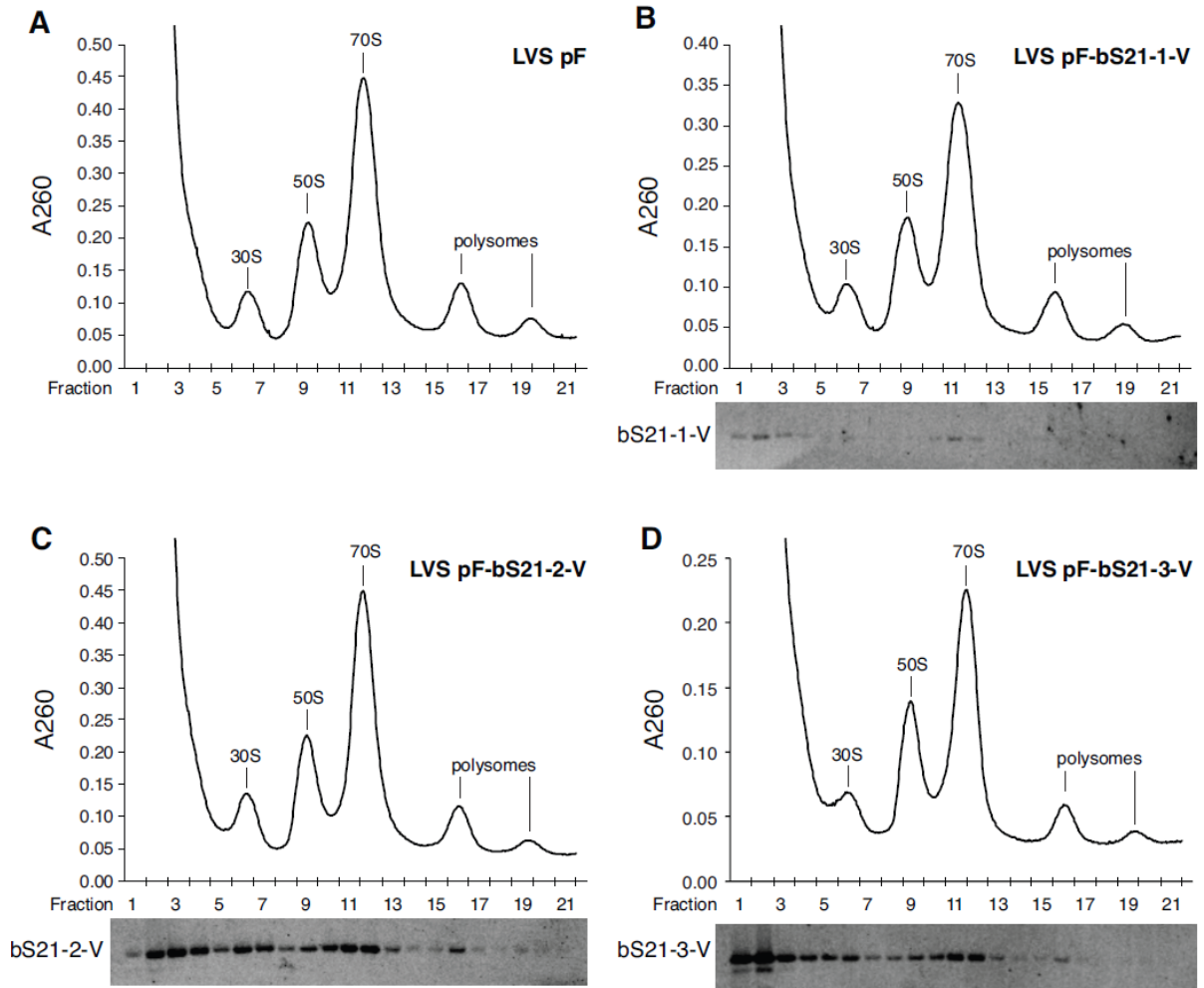


**Figure S3. Each bS21 homolog can be detected in translationally-active ribosomes.** For **A – D**, top: Sucrose gradient sedimentation profile from actively-translating wild-type *F. tularensis* cells with either empty vector or ectopic expression of indicated bS21 homolog. Nucleic acid content was monitored by A260 (y-axis). Peaks corresponding to the 30S, 50S, 70S, and polysomes are indicated. Fractions collected are indicated on the x-axis. For **A – D**, bottom: Immunoblot analysis of fractions from sucrose gradient sedimentation (above), probing for VSV-G. Wells correspond to fractions 1 – 21 from profile above. **A.** Cells from wild-type *F. tularensis* LVS with empty vector (LVS pF). **B.** Cells from wild-type *F. tularensis* LVS with ectopic expression of bS21-1 (LVS pF-bS21-1-V). **C.** Cells from wild-type *F. tularensis* LVS with ectopic expression of bS21-2 (LVS pF-bS21-2-V). **D.** Cells from wild-type *F. tularensis* LVS with ectopic expression of bS21-3 (LVS pF-bS21-3-V).

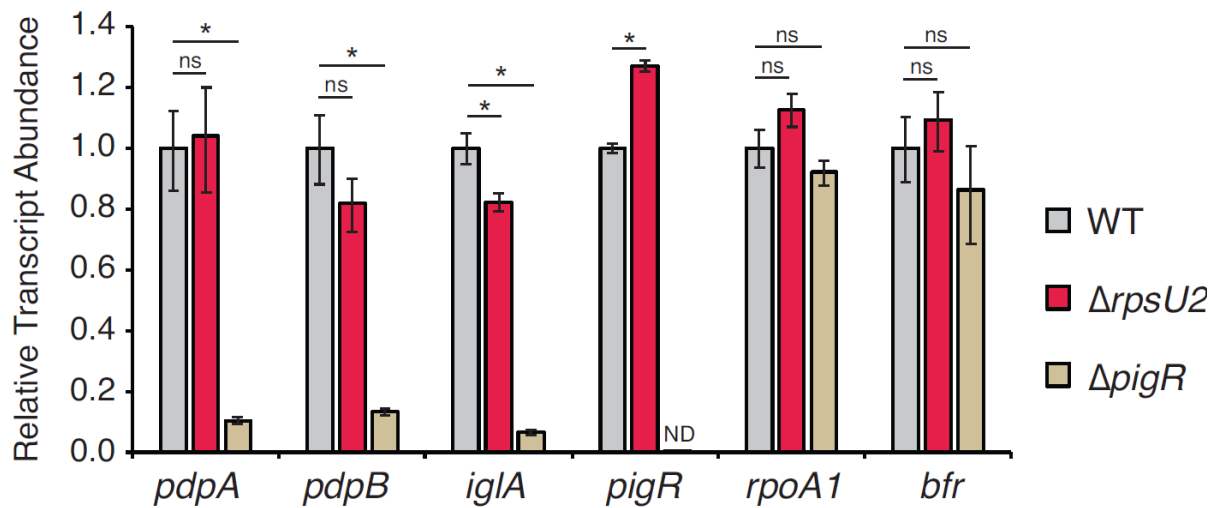


**Figure S4. Loss of bS21-2 does not affect transcript abundance of FPI-encoded genes.** Quantitative real-time PCR was used to determine the relative transcript abundance for indicated FPI genes in wild-type cells, cells lacking bS21-2 ( $\Delta rpsU2$ ), or cells lacking the transcription factor PigR ( $\Delta pigR$ ). Cells lacking PigR serve as a positive control, as PigR positively regulates its own transcription and the transcription of *pdpA*, *pdpB*, and *iglA*. The *rpoA1* and *bfr* genes are included as negative controls, as their expression is not influenced by bS21-2 or PigR. Transcript abundances are normalized to *tul4*, whose expression is not influenced by bS21-2 or PigR. Error bars represent 1 SD from the value (calculated using the mean threshold cycle). ns: not significant. ND: not detected \*adjusted  $p < 0.05$  by t-test with Bonferroni correction.

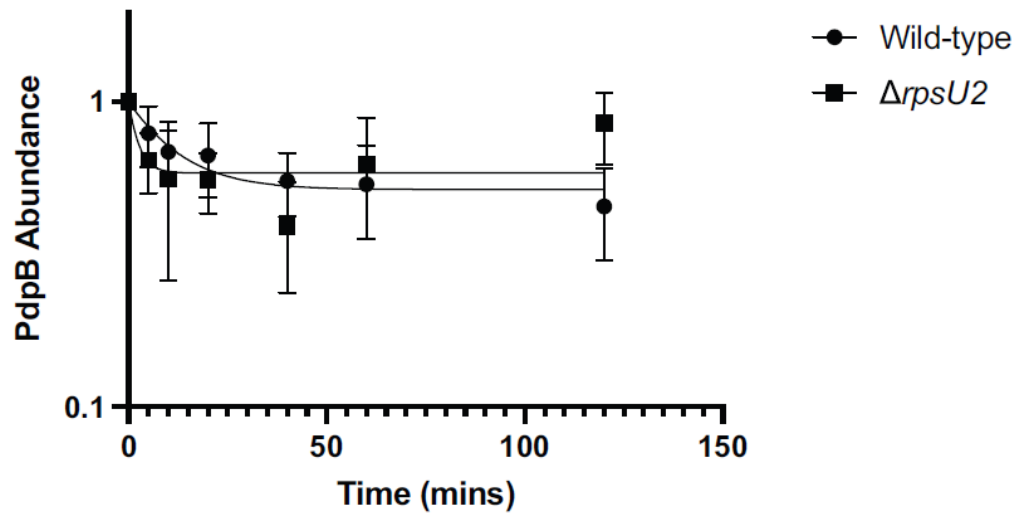


**Figure S5. Loss of bS21-2 does not affect protein degradation of PdpB.** One-phase decay of PdpB from antibiotic-chase experiment from wild-type cells and cells lacking bS21-2 ( $\Delta rpsU2$ ). Neither strain showed significant degradation of PdpB through the time points assessed; the calculated half-life for both was greater than 120 minutes. Y-axis is logarithmic and error bars represent 1 SD from the mean.

Supplemental Tables S1, S2, and S3 can be found in Appendix 1

**Table S4.** Comparison of *in vitro* and intramacrophage growth rates for strains used in this study. *In vitro* growth was assessed during early exponential phase by measuring OD600. *In vitro* generation times for LVS pF, LVS  $\Delta rpsU2$  pF, and LVS  $\Delta rpsU2$  pF-bS21-2-V were calculated from three independent experiments, others were calculated from two. Generation times for intramacrophage growth are averages across three independent experiments and were determined by comparison of CFU recovered after 2 versus 24 hours. +/- values indicate SD.

Cells	Growth environment		Generation time difference (intramacrophage - <i>in vitro</i> )
	<i>in vitro</i>	Intramacrophage	
LVS pF	135.1 +/- 4.7	144.8 +/- 7.1	9.7
LVS $\Delta rpsU2$ pF	172.8 +/- 4.5	210.7 +/- 29.5	37.9
LVS $\Delta rpsU2$ pF- bS21-1-V	145.1 +/- 3.9	179.3 +/- 8.2	34.2
LVS $\Delta rpsU2$ pF- bS21-2-V	150.6 +/- 1.9	144.5 +/- 5.0	-6.1
LVS $\Delta rpsU2$ pF- bS21-2-V	181.2 +/- 7.6	263.1 +/- 20.3	81.9

## Supplemental References

1. Lupski JR, Godson GN. 1984. The *rpsU-dnaG-rpoD* macromolecular synthesis operon of *E. coli*. Cell 39:251–252.
2. Madeira F, Pearce M, Tivey ARN, Basutkar P, Lee J, Edbali O, Madhusoodanan N, Kolesnikov A, Lopez R. 2022. Search and sequence analysis tools services from EMBL-EBI in 2022. Nucleic Acids Res 50:W276–W279.